Measurement of the CP asymmetry in $B_s^0 - \overline{B}_s^0$ mixing

LHCb Collaboration; Bernet, R; Müller, K; Steinkampf, O; Straumann, U; Vollhardt, A; et al

Abstract: The CP asymmetry in the mixing of B_s^0 and $\overline{B}_s^0$ mesons is measured in proton-proton collision data corresponding to an integrated luminosity of 3.0 fb^{-1}, recorded by the LHCb experiment at centre-of-mass energies of 7 and 8 TeV. Semileptonic B_s^0 and $\overline{B}_s^0$ decays are studied in the inclusive mode $D_s^{\mp}\mu^{\pm}\nu_{\mu}X$ with the $D_s^{\mp}$ mesons reconstructed in the $K^+K^-\pi^{\mp}$ final state. Correcting the observed charge asymmetry for detection and background effects, the CP asymmetry is found to be $a_{\rm sl}^s = (0.39 \pm 0.26 \pm 0.20)$

DOI: https://doi.org/10.1103/PhysRevLett.117.061803

Measurement of the *CP* Asymmetry in $B_s^0 - \bar{B}_s^0$ Mixing

R. Aaij *et al.*[*]
(LHCb Collaboration)

(Received 1 June 2016; published 5 August 2016)

The *CP* asymmetry in the mixing of B_s^0 and $\bar{B}_s^0$ mesons is measured in proton-proton collision data corresponding to an integrated luminosity of 3.0 fb^{-1}, recorded by the LHCb experiment at center-of-mass energies of 7 and 8 TeV. Semileptonic B_s^0 and $\bar{B}_s^0$ decays are studied in the inclusive mode $D_s^{\mp}\mu^{\pm}\overset{(-)}{\nu}_{\mu}X$ with the $D_s^{\mp}$ mesons reconstructed in the $K^+K^-\pi^{\mp}$ final state. Correcting the observed charge asymmetry for detection and background effects, the *CP* asymmetry is found to be $a_{\rm sl}^s = (0.39 \pm 0.26 \pm 0.20)\%$, where the first uncertainty is statistical and the second systematic. This is the most precise measurement of $a_{\rm sl}^s$ to date. It is consistent with the prediction from the standard model and will constrain new models of particle physics.

DOI: 10.1103/PhysRevLett.117.061803

When neutral B mesons evolve in time they can change into their own antiparticles. This quantum-mechanical phenomenon is known as mixing and occurs in both neutral B meson systems, B^0 and B_s^0, where B is used to refer to either system. In this mixing process, the *CP* (charge-parity) symmetry is broken if the probability for a B meson to change into a $\bar{B}$ meson is different from the probability for the reverse process. This effect can be measured by studying decays into flavor-specific final states, $B \to f$, such that $\bar{B} \to f$ transitions can only occur through the mixing process $\bar{B} \to B \to f$. Such processes include semileptonic B decays, as the charge of the lepton identifies the flavor of the B meson at the time of its decay. The magnitude of the *CP*-violating asymmetry in B mixing can be characterized by the semileptonic asymmetry $a_{\rm sl}$. This is defined in terms of the partial decay rates, Γ, to semileptonic final states as

$$a_{\rm sl} \equiv \frac{\Gamma(\bar{B} \to f) - \Gamma(B \to \bar{f})}{\Gamma(\bar{B} \to f) + \Gamma(B \to \bar{f})} \approx \frac{\Delta\Gamma}{\Delta m}\tan\phi_{12}, \qquad (1)$$

where Δm ($\Delta\Gamma$) is the difference in mass (decay width) between the mass eigenstates of the B system and ϕ_{12} is a *CP*-violating phase [1]. In the standard model (SM), the asymmetry is predicted to be as small as $a_{\rm sl}^d = (-4.7 \pm 0.6) \times 10^{-4}$ in the B^0 system and $a_{\rm sl}^s = (2.22 \pm 0.27) \times 10^{-5}$ in the B_s^0 system [1,2]. However, these values may be enhanced by non-SM contributions to the mixing process [3].

Measurements of $a_{\rm sl}$ have led to an inconclusive picture. In 2010, the D0 Collaboration reported an anomalous charge asymmetry in the inclusive production rates of like-sign dimuons [4], which is sensitive to a combination of $a_{\rm sl}^d$ and $a_{\rm sl}^s$. Their most recent study shows a discrepancy with SM predictions of about 3 standard deviations [5]. The current experimental world averages, excluding the anomalous D0 result, are $a_{\rm sl}^d = (0.01 \pm 0.20)\%$ and $a_{\rm sl}^s = (-0.48 \pm 0.48)\%$ [6], compatible with both the SM predictions and the D0 measurement. The measurement of $a_{\rm sl}^s$ presented in this Letter is based on data recorded by LHCb in 2011 and 2012, corresponding to an integrated luminosity of 3.0 fb^{-1}. It supersedes the previous LHCb measurement [7], which used the 1.0 fb^{-1} data sample taken in 2011. Semileptonic decays $B_s^0 \to D_s^-\mu^+\nu_\mu X$, where X represents any number of particles, are reconstructed inclusively in $D_s^-\mu^+$. Charge-conjugate modes are implied throughout, except in the definitions of charge asymmetry. The D_s^- meson is reconstructed in the $K^+K^-\pi^-$ final state. This analysis extends the previous LHCb measurement, which considered only $D_s^- \to \phi\pi^-$ decays, by including all possible D_s^- decays to the $K^+K^-\pi^-$ final state.

Starting from a sample with equal numbers of B_s^0 and $\bar{B}_s^0$ mesons, $a_{\rm sl}^s$ can be measured without determining (tagging) the initial flavor. The raw asymmetry of observed $D_s^-\,\mu^+$ and $D_s^+\,\mu^-$ candidates, integrated over B_s^0 decay time, is

$$A_{\rm raw} = \frac{N(D_s^-\mu^+) - N(D_s^+\mu^-)}{N(D_s^-\mu^+) + N(D_s^+\mu^-)}. \qquad (2)$$

The high oscillation frequency Δm_s reduces the effect of the small asymmetry in the production rates between B_s^0 and $\bar{B}_s^0$ mesons in pp collisions by a factor 10^{-3} [7,8]. Neglecting corrections, the untagged, time-integrated asymmetry is $A_{\rm raw} = a_{\rm sl}^s/2$, where the factor 2 reduction compared to the tagged asymmetry in Eq. (1) comes from the summation over mixed and unmixed decays. The tagged asymmetry would actually suffer from a larger

[*]Full author list given at the end of the article.

reduction because of the tagging efficiency [9,10]. The unmixed decays have zero asymmetry due to CPT symmetry. The raw asymmetry is still affected by possible differences in detection efficiency for the two charge-conjugate final states and by backgrounds from other b-hadron decays to $D_s^- \mu^+ X$. Hence, $a_{\rm sl}^s$ is calculated as

$$a_{\rm sl}^s = \frac{2}{1 - f_{\rm bkg}} (A_{\rm raw} - A_{\rm det} - f_{\rm bkg} A_{\rm bkg}), \qquad (3)$$

where $A_{\rm det}$ is the detection asymmetry, which is assessed from data using calibration samples, $f_{\rm bkg}$ is the fraction of the b-hadron background, and $A_{\rm bkg}$ the background asymmetry.

The LHCb detector is a single-arm forward spectrometer designed for the study of particles containing b or c quarks [11,12]. A high-precision tracking system with a dipole magnet measures the momentum (p) and impact parameter (IP) of charged particles. The IP is defined as the distance of closest approach between the track and any primary proton-proton interaction and is used to distinguish between D_s^- mesons from B decays and D_s^- mesons promptly produced in the primary interaction. The regular reversal of the magnet polarity allows a quantitative assessment of detector-induced charge asymmetries. Different types of charged particles are distinguished using particle identification (PID) information from two ring-imaging Cherenkov detectors, an electromagnetic calorimeter, a hadronic calorimeter and a muon system. Online event selection is performed by a two-stage trigger. For this analysis, the first (hardware) stage selects muons in the muon system; the second (software) stage applies a full event reconstruction. Here the events are first selected by the presence of the muon or one of the hadrons from the D_s^- decay, after which a combination of the decay products is required to be consistent with the topological signature of a b-hadron decay. Simulated events are produced using the software described in Refs. [13–17].

Different intermediate states, clearly visible in the Dalitz plot shown in Fig. 1, contribute to the three-body $D_s^- \to K^+K^-\pi^-$ decays. Three disjoint regions are defined, which have different levels of background. The $\phi\pi$ region is the cleanest and is selected by requiring the reconstructed K^+K^- mass to be within ± 20 MeV$/c^2$ of the known ϕ mass. The K^*K region is selected by requiring the reconstructed $K^+\pi^-$ mass to be within ± 90 MeV$/c^2$ of the known $K^*(892)^0$ mass. The remaining D_s^- candidates are included in the non-resonant (NR) region, which also covers other intermediate states [18].

The D_s^- candidates are reconstructed from three charged tracks, and then a muon track with opposite charge is added. All four tracks are required to have a good quality track fit and significant IP. The contribution from prompt D_s^- background is suppressed to a negligible level by imposing a lower bound on the IP of the D_s^- candidates.

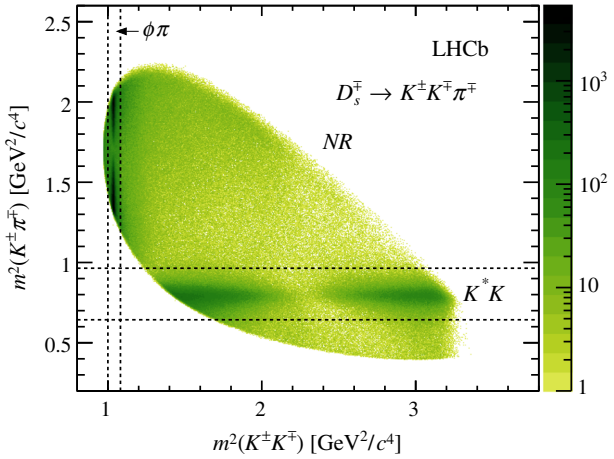

FIG. 1. Dalitz plot of the $D_s^\mp \to K^\pm K^\mp \pi^\mp$ decay for selected $D_s^\mp \mu^\pm$ candidates, with the three selection regions indicated. To suppress combinatorial background, a narrow invariant mass window, between 1950 and 1990 MeV$/c^2$, is required for the $D_s^\mp$ candidates in this plot.

To ensure a good overlap with the calibration samples, minimum momenta of 2, 5, and 6 GeV$/c$ and minimum transverse momenta, p_T, of 300, 400, and 1200 MeV$/c$ are required for the pions, kaons, and muons, respectively. To suppress background, kaon and pion candidates are required to be positively identified by the PID system. Candidates are selected by requiring a good quality of the D_s^- and B_s^0 decay vertices. A source of background arises from D_s^- candidates where one of the three decay particles is misidentified. The main contributions are from $\bar{\Lambda}_c^- \to K^+\bar{p}\pi^-$, $D^- \to K^+\pi^-\pi^-$, $J/\psi X$, and misidentified or partially reconstructed multibody D decays, all originating from semileptonic b-hadron decays. They are suppressed to a negligible level by specific vetoes, which apply tight PID requirements in a small window of invariant mass of the corresponding particle combination. These vetoes are optimized separately for each Dalitz plot region. To check that this does not introduce additional asymmetries, these selections are applied to control samples of promptly produced D_s^- mesons. The asymmetries are found to be consistent between the Dalitz regions.

The $D_s^- \mu^+$ signal yields are obtained from fits to the $K^+K^-\pi^-$ invariant mass distributions. These yields contain contributions from backgrounds that also peak at the D_s^- mass, originating from other b-hadron decays into D_s^- mesons and muons. Simulation studies indicate that these peaking backgrounds are mainly composed of b-hadron decays to $D_s^- X_c X$, where the D_s^- meson originates from a $b \to c\bar{c}s$ transition, and X_c is a charmed hadron decaying semileptonically.

An example of such a background is $B^- \to D_s^- \bar{D}^0 X$. Other, smaller contributors are $B^+ \to D_s^- K^+ \mu^+ \nu_\mu X$ and $B^0 \to D_s^- K_S^0 \mu^+ \nu_\mu X$ decays. All of these peaking backgrounds have more missing particles than the

$B_s^0 \to D_s^- \mu^+ \nu_\mu X$ signal decay. Their contribution is reduced by requiring the corrected B_s^0 mass, defined as $m_{\rm corr} \equiv \sqrt{m^2 + p_T^2} + p_T$, to be larger than 4200 MeV/c^2, where m is the $D_s^- \mu^+$ invariant mass and p_T the $D_s^- \mu^+$ momentum transverse to the line connecting the primary and B_s^0 decay vertices.

The estimates of $f_{\rm bkg}$ and $A_{\rm bkg}$ are based on known branching fractions [18], selection efficiencies, and background asymmetries, using a similar approach as in the previous measurement [7]. The reconstruction and selection efficiencies of the backgrounds relative to the signal efficiency are determined from simulation. The total background asymmetry is given by the sum of all contributions as $f_{\rm bkg} A_{\rm bkg} \equiv \sum_i f^i_{\rm bkg} A^i_{\rm bkg}$. The background asymmetries mainly originate from the production asymmetries of b hadrons. The production asymmetry between B^+ and B^- mesons is $A_{\rm bkg}(B^+) = (-0.6 \pm 0.6)\%$, obtained from the observed asymmetry in $B^+ \to J/\psi K^+$ decays [19], after correcting for the kaon detection asymmetry and the direct CP asymmetry [18]. For the B^0 background, there are contributions from the production asymmetry and from $a^d_{\rm sl}$ [20]. Both asymmetries are diluted when integrating over the B^0 decay time, resulting in $A_{\rm bkg}(B^0) = (-0.18 \pm 0.13)\%$. The production asymmetry in the Λ_b^0 backgrounds is estimated based on the combined CP and production asymmetry measured in $\Lambda_b^0 \to J/\psi p^+ K^-$ decays [21]. The direct CP asymmetry in this decay mode is estimated to be $(-0.6 \pm 0.3)\%$, using the measurements in Ref. [22] and the method proposed in Ref. [23]. Subtracting this from the combined asymmetry [21] results in $A_{\rm bkg}(\Lambda_b^0) = (+0.5 \pm 0.8)\%$. The overall peaking background fraction is $f_{\rm bkg} = (18.4 \pm 6.0)\%$ and the correction for the background asymmetry is $f_{\rm bkg} A_{\rm bkg} = (-0.023 \pm 0.031)\%$.

The $K^+K^-\pi^\mp$ mass distributions are shown in Fig. 2, with the fit results superimposed. The $D_s^\mp\ \mu^\pm$ yields are found to be 899×10^3 in the $\phi\pi$ region, 413×10^3 in the K^*K region, and 280×10^3 in the NR region. Extended maximum likelihood fits are made separately for the three Dalitz regions, for the two magnet polarities, and the two data-taking periods (2011 and 2012). To accurately determine the background shape from random combinations of $K^+K^-\pi^-$ candidates, a wide mass window between 1800 and 2047 MeV/c^2 is used, which includes the Cabibbo-suppressed $D^- \to K^+K^-\pi^-$ decay. Both peaks are modeled with a double-sided Hypatia function [24]. The tail parameters of this function are determined for each Dalitz region by a fit to the combined data sets for all magnet polarities and data-taking periods, and subsequently fixed in the twelve individual mass fits. A systematic uncertainty is assigned to account for fixing these parameters. The combinatorial background is modelled with a second-order polynomial. A simultaneous fit to the $m(K^+K^-\pi^-)$ and $m(K^+K^-\pi^+)$ distributions is performed. All signal parameters except the mean masses and signal yields are shared between the D_s^- and D_s^+ candidates. All background parameters vary independently in the fit to allow for any asymmetry in the combinatorial background. Possible biases from the fit model are studied by generating invariant mass distributions with the signal component described by a double Gaussian function with power-law tails on both sides, and subsequently applying the fit with the default Hypatia shape. The change in the value of $A_{\rm raw}$ is assigned as a systematic uncertainty.

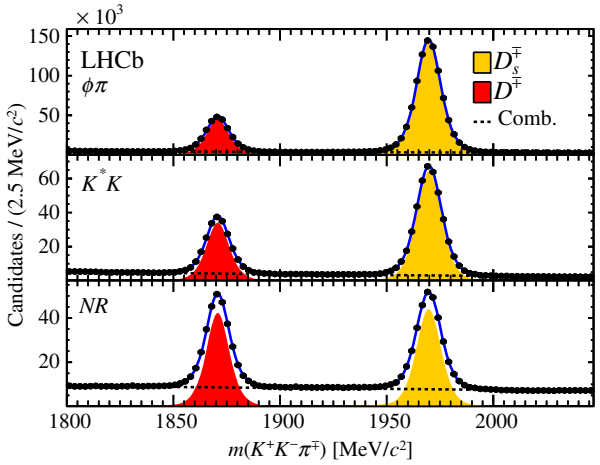

FIG. 2. Distributions of $K^+K^-\pi^\mp$ mass in the three Dalitz plot regions, summed over both magnet polarities and data-taking periods. Overlaid is the result of the fit, with signal and combinatorial background components as indicated in the legend.

Asymmetries are averaged as follows. For each magnet polarity and data-taking period, the weighted average of the asymmetries of the three Dalitz regions is taken. Then the arithmetic average for the two magnet polarities is taken to minimize possible residual detection asymmetries [7]. Finally, a weighted average is made over the two data-taking periods. The resulting raw asymmetry is $A_{\rm raw} = (0.11 \pm 0.09)\%$.

The asymmetry $A_{\rm det}$, arising from the difference in detection efficiencies between the $D_s^-\ \mu^+$ and $D_s^+\ \mu^-$ candidates, is determined using calibration samples. The asymmetry is split up as

$$A_{\rm det} = A_{\rm track} + A_{\rm PID} + A_{\rm trig}, \tag{4}$$

where the individual contributions are described below. For each calibration sample, event weights are applied to match the three-momentum distributions of the calibration particles to those of the signal decays. The weights are determined in bins of the distributions of momenta and angles. Alternative binning schemes are used to assess the systematic uncertainties due to the weighting procedure.

The track reconstruction asymmetry, $A_{\rm track}$, is split into a contribution, $A_{\rm track}(K^+K^-)$, associated with the reconstruction of the K^+K^- pair and a contribution, $A_{\rm track}(\pi^-\mu^+)$, associated with the $\pi^-\mu^+$ pair. The track

reconstruction efficiency for single kaons suffers from a sizeable difference between K^+ and K^- cross sections with the detector material, which depends on the kaon momentum. This asymmetry largely cancels in $A_{\rm track}(K^+K^-)$ due to the similar kinematic distributions of the positive and negative kaons. The kaon asymmetry is calculated using prompt $D^- \to K^+\pi^-\pi^-$ and $D^- \to K^0_S\pi^-$ decays, similarly to Refs. [20,25]. For pions and muons, the charge asymmetry due to interactions in the detector material is assumed to be negligible, and a systematic uncertainty is assigned for this assumption [20]. Effects from the track reconstruction algorithms and detector acceptance, combined with a difference in kinematic distributions between pions and muons, can result in a charge asymmetry. It is assessed here with two methods. The first method measures the track reconstruction efficiency using samples of partially reconstructed $J/\psi \to \mu^+\mu^-$ decays as described in Ref. [26]. The second method uses fully and partially reconstructed $D^{*-} \to \bar{D}^0(K^+\pi^-\pi^+\pi^-)\pi^-$ decays as described in Ref. [27]. The final value of $A_{\rm track}(\pi^-\mu^+)$ is obtained as the weighted average from the two methods. The systematic uncertainty on this number includes a small effect from differences in the detector acceptance for positive and negative particles.

The asymmetry induced by the PID requirements, $A_{\rm PID}$, is determined using large samples of $D^{*+} \to D^0(K^-\pi^+)\pi^+$ and $J/\psi \to \mu^+\mu^-$ decays. The D^{*+} charge identifies the kaon and the pion of the D^0 decay without the use of PID requirements, which is then used to determine the PID efficiencies and corresponding charge asymmetries.

The asymmetry induced by the trigger, $A_{\rm trig}$, is split into contributions from the muon hardware trigger and from the software trigger. The first, $A_{\rm trig}(\text{hardware})$, is assessed using samples of $J/\psi \to \mu^+\mu^-$ decays in data. The second, $A_{\rm trig}(\text{software})$, is mainly caused by the trigger requirements on the muon or one of the hadrons from the D_s^- decay. The asymmetry from the muon software trigger is determined in a similar fashion to that from the hardware trigger. The asymmetry due to the trigger requirement on the hadrons is determined using samples of prompt $D_s^- \to K^+K^-\pi^-$ decays that have been triggered by other particles in the event. The combined asymmetry takes into account the overlap between the two triggers.

The measured values of all detection asymmetries with their statistical and systematic uncertainties are shown in Table I. The overall corrections are small and compatible with zero. In contrast, corrections for separate magnet polarities are more significant (at most 1.1% in 2011 and 0.3% in 2012), as expected for most of the detector-induced charge asymmetries. The corrections for the detection asymmetries are almost fully correlated between the Dalitz regions.

The previous analysis, based on 1.0 fb^{-1}, used only candidates in the $\phi\pi$ region of the Dalitz plot, with different selection criteria, and used a different fit method to determine the signal yields [7]. A more stringent selection resulted in a cleaner signal sample, but with roughly 30% fewer signal candidates in the $\phi\pi$ region. As a cross-check, the approach of the previous analysis is repeated on the full 3.0 fb^{-1} data sample and the result is compatible within 1 standard deviation.

TABLE I. Overview of contributions in the determination of $a^s_{\rm sl}$, averaged over Dalitz plot regions, magnet polarities, and data taking periods, with their statistical and systematic uncertainties. All numbers are in percent. The central value of $a^s_{\rm sl}$ is calculated according to Eq. (3). The uncertainties are added in quadrature and multiplied by $2/(1-f_{\rm bkg})$, which is the same for all twelve subsamples, to obtain the uncertainties on $a^s_{\rm sl}$.

Source	Value	Statistical uncertainties	Systematic uncertainties	
$A_{\rm raw}$	0.11	0.09	0.02	
$-A_{\rm track}(K^+K^-)$	0.01	0.00	0.03	
$-A_{\rm track}(\pi^-\mu^+)$	0.01	0.05	0.04	
$-A_{\rm PID}$	−0.01	0.02	0.03	
$-A_{\rm trig}(\text{hardware})$	0.03	0.02	0.02	
$-A_{\rm trig}(\text{software})$	0.00	0.01	0.02	
$-f_{\rm bkg}\ A_{\rm bkg}$	0.02	–	0.03	+
$(1-f_{\rm bkg})a^s_{\rm sl}/2$	0.16	0.11	0.08	
$2/(1-f_{\rm bkg})$	2.45	–	0.18	×
$a^s_{\rm sl}$	0.39	0.26	0.20	

The twelve values of $a^s_{\rm sl}$ for each Dalitz region, polarity, and data-taking period are consistent with each other. The combined result, taking into account all correlations, is

$$a^s_{\rm sl} = (0.39 \pm 0.26 \pm 0.20)\%,$$

where the first uncertainty is statistical, originating from the size of the signal and calibration samples, and the

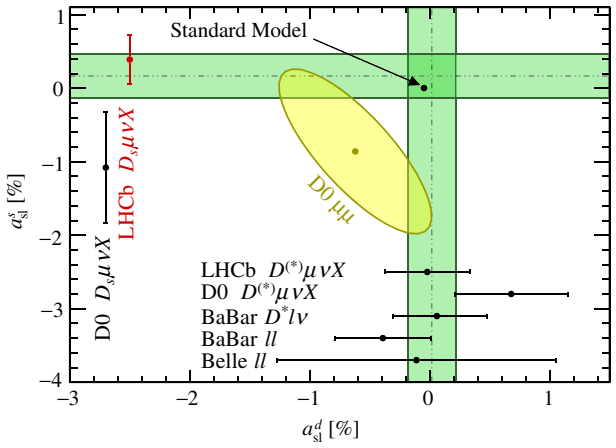

FIG. 3. Overview of the most precise measurements of $a^d_{\rm sl}$ and $a^s_{\rm sl}$. The horizontal and vertical bands indicate the naive averages of pure $a^s_{\rm sl}$ and $a^d_{\rm sl}$ measurements [20,28–32]. The yellow ellipse represents the D0 dimuon measurement with $\Delta\Gamma_d/\Gamma_d$ set to its SM expectation value [5]. The error bands and contours correspond to a 68% confidence level.

second systematic. There is a small correlation coefficient of +0.13 between this measurement and the LHCb measurement of $a^d_{\rm sl}$ [20]. The correlation mainly originates from the muon detection asymmetry and from the effect of $a^d_{\rm sl}$, due to B^0 background, on the measurement of $a^s_{\rm sl}$. Figure 3 displays an overview of the most precise measurements of $a^d_{\rm sl}$ and $a^s_{\rm sl}$ [5,20,28–32]. The simple averages of pure $a_{\rm sl}$ measurements, including the present $a^s_{\rm sl}$ result and accounting for the small correlation from LHCb, are found to be $a^d_{\rm sl} = (0.02 \pm 0.20)\%$ and $a^s_{\rm sl} = (0.17 \pm 0.30)\%$ with a correlation of +0.07. In combination, these two averages are marginally compatible with the D0 dimuon result ($p = 0.5\%$) shown in Fig. 3. In summary, the determination of $a^s_{\rm sl}$ presented in this Letter is the most precise to date. It shows no evidence for new physics effects and will serve to restrict models beyond the SM.

We express our gratitude to our colleagues in the CERN accelerator departments for the excellent performance of the LHC. We thank the technical and administrative staff at the LHCb institutes. We acknowledge support from CERN and from the national agencies: CAPES, CNPq, FAPERJ, and FINEP (Brazil); NSFC (China); CNRS/IN2P3 (France); BMBF, DFG, and MPG (Germany); INFN (Italy); FOM and NWO (Netherlands); MNiSW and NCN (Poland); MEN/IFA (Romania); MinES and FANO (Russia); MinECo (Spain); SNSF and SER (Switzerland); NASU (Ukraine); STFC (United Kingdom); NSF (USA). We acknowledge the computing resources that are provided by CERN, IN2P3 (France), KIT and DESY (Germany), INFN (Italy), SURF (Netherlands), PIC (Spain), GridPP (United Kingdom), RRCKI and Yandex LLC (Russia), CSCS (Switzerland), IFIN-HH (Romania), CBPF (Brazil), PL-GRID (Poland), and OSC Ohio Supercomputer Center(USA). We are indebted to the communities behind the multiple open source software packages on which we depend. Individual groups or members have received support from the AvH Foundation (Germany), EPLANET, Marie Skłodowska-Curie Actions, and ERC (European Union), Conseil Général de Haute-Savoie, Labex ENIGMASS, and OCEVU, Région Auvergne (France), RFBR and Yandex LLC (Russia), GVA, XuntaGal, and GENCAT (Spain), Herchel Smith Fund, The Royal Society, Royal Commission for the Exhibition of 1851, and the Leverhulme Trust (United Kingdom).

[1] A. Lenz and U. Nierste, J. High Energy Phys. 06 (2007) 072.
[2] M. Artuso, G. Borissov, and A. Lenz, arXiv:1511.09466 [Rev. Mod. Phys. (to be published)].
[3] A. Lenz, U. Nierste, J. Charles, S. Descotes-Genon, H. Lacker, S. Monteil, V. Niess, and S. T'Jampens, Phys. Rev. D **86**, 033008 (2012).
[4] V. Abazov *et al.* (D0 Collaboration), Phys. Rev. Lett. **105**, 081801 (2010).
[5] V. M. Abazov *et al.* (D0 Collaboration), Phys. Rev. D **89**, 012002 (2014).
[6] Y. Amhis *et al.* (Heavy Flavor Averaging Group), arXiv: 1412.7515; updated results and plots available at http://www.slac.stanford.edu/xorg/hfag/.
[7] R. Aaij *et al.* (LHCb Collaboration), Phys. Lett. B **728**, 607 (2014).
[8] R. Aaij *et al.* (LHCb Collaboration), Phys. Lett. B **739**, 218 (2014).
[9] R. Aaij *et al.* (LHCb Collaboration), Eur. Phys. J. C **72**, 2022 (2012).
[10] R. Aaij *et al.* (LHCb Collaboration), J. Instrum. **11**, P05010 (2016).
[11] A. A. Alves, Jr. *et al.* (LHCb Collaboration), J. Instrum. **3**, S08005 (2008).
[12] R. Aaij *et al.* (LHCb Collaboration), Int. J. Mod. Phys. A **30**, 1530022 (2015).
[13] T. Sjöstrand, S. Mrenna, and P. Skands, J. High Energy Phys. 05 (2006) 026; Comput. Phys. Commun. **178**, 852 (2008).
[14] I. Belyaev *et al.*, J. Phys. Conf. Ser. **331**, 032047 (2011).
[15] D. J. Lange, Nucl. Instrum. Methods Phys. Res., Sect. A **462**, 152 (2001).
[16] J. Allison, K. Amako, J. Apostolakis, H. Araujo, P. Dubois *et al.* (Geant4 Collaboration), IEEE Trans. Nucl. Sci. **53**, 270 (2006); S. Agostinelli *et al.* (Geant4 Collaboration), Nucl. Instrum. Methods Phys. Res., Sect. A **506**, 250 (2003).
[17] M. Clemencic, G. Corti, S. Easo, C. R. Jones, S. Miglioranzi, M. Pappagallo, and P. Robbe, J. Phys. Conf. Ser. **331**, 032023 (2011).
[18] K. A. Olive *et al.* (Particle Data Group), Chin. Phys. C **38**, 090001 (2014); and 2015 update.
[19] R. Aaij *et al.* (LHCb Collaboration), J. High Energy Phys. 09 (2014) 177.
[20] R. Aaij *et al.* (LHCb Collaboration), Phys. Rev. Lett. **114**, 041601 (2015).
[21] R. Aaij *et al.* (LHCb Collaboration), Chin. Phys. C **40**, 011001 (2016).
[22] R. Aaij *et al.* (LHCb Collaboration), J. High Energy Phys. 07 (2014) 103.
[23] K. De Bruyn and R. Fleischer, J. High Energy Phys. 03 (2015) 145.
[24] D. Martinez Santos and F. Dupertuis, Nucl. Instrum. Methods Phys. Res., Sect. A **764**, 150 (2014).
[25] R. Aaij *et al.* (LHCb Collaboration), J. High Energy Phys. 07 (2014) 041.
[26] R. Aaij *et al.* (LHCb Collaboration), J. Instrum. **10**, P02007 (2015).
[27] R. Aaij *et al.* (LHCb Collaboration), Phys. Lett. B **713**, 186 (2012).
[28] E. Nakano *et al.* (Belle Collaboration), Phys. Rev. D **73**, 112002 (2006).

[29] J. P. Lees *et al.* (*BABAR* Collaboration), Phys. Rev. Lett. **111**, 101802 (2013).
[30] J. P. Lees *et al.* (*BABAR* Collaboration), Phys. Rev. Lett. **114**, 081801 (2015).
[31] V. M. Abazov *et al.* (D0 Collaboration), Phys. Rev. D **86**, 072009 (2012).
[32] V. Abazov *et al.* (D0 Collaboration), Phys. Rev. Lett. **110**, 011801 (2013).

R. Aaij,[39] B. Adeva,[38] M. Adinolfi,[47] Z. Ajaltouni,[5] S. Akar,[6] J. Albrecht,[10] F. Alessio,[39] M. Alexander,[52] S. Ali,[42] G. Alkhazov,[31] P. Alvarez Cartelle,[54] A. A. Alves Jr.,[58] S. Amato,[2] S. Amerio,[23] Y. Amhis,[7] L. An,[40] L. Anderlini,[18] G. Andreassi,[40] M. Andreotti,[17,a] J. E. Andrews,[59] R. B. Appleby,[55] O. Aquines Gutierrez,[11] F. Archilli,[1] P. d'Argent,[12] J. Arnau Romeu,[6] A. Artamonov,[36] M. Artuso,[60] E. Aslanides,[6] G. Auriemma,[26,b] M. Baalouch,[5] S. Bachmann,[12] J. J. Back,[49] A. Badalov,[37] C. Baesso,[61] W. Baldini,[17] R. J. Barlow,[55] C. Barschel,[39] S. Barsuk,[7] W. Barter,[39] V. Batozskaya,[29] V. Battista,[40] A. Bay,[40] L. Beaucourt,[4] J. Beddow,[52] F. Bedeschi,[24] I. Bediaga,[1] L. J. Bel,[42] V. Bellee,[40] N. Belloli,[21,c] K. Belous,[36] I. Belyaev,[32] E. Ben-Haim,[8] G. Bencivenni,[19] S. Benson,[39] J. Benton,[47] A. Berezhnoy,[33] R. Bernet,[41] A. Bertolin,[23] M.-O. Bettler,[39] M. van Beuzekom,[42] S. Bifani,[46] P. Billoir,[8] T. Bird,[55] A. Birnkraut,[10] A. Bitadze,[55] A. Bizzeti,[18,d] T. Blake,[49] F. Blanc,[40] J. Blouw,[11] S. Blusk,[60] V. Bocci,[26] T. Boettcher,[57] A. Bondar,[35] N. Bondar,[31,39] W. Bonivento,[16] S. Borghi,[55] M. Borisyak,[67] M. Borsato,[38] F. Bossu,[7] M. Boubdir,[9] T. J. V. Bowcock,[53] E. Bowen,[41] C. Bozzi,[17,39] S. Braun,[12] M. Britsch,[12] T. Britton,[60] J. Brodzicka,[55] E. Buchanan,[47] C. Burr,[55] A. Bursche,[2] J. Buytaert,[39] S. Cadeddu,[16] R. Calabrese,[17,a] M. Calvi,[21,c] M. Calvo Gomez,[37,e] P. Campana,[19] D. Campora Perez,[39] L. Capriotti,[55] A. Carbone,[15,f] G. Carboni,[25,g] R. Cardinale,[20,h] A. Cardini,[16] P. Carniti,[21,c] L. Carson,[51] K. Carvalho Akiba,[2] G. Casse,[53] L. Cassina,[21,c] L. Castillo Garcia,[40] M. Cattaneo,[39] Ch. Cauet,[10] G. Cavallero,[20] R. Cenci,[24,i] M. Charles,[8] Ph. Charpentier,[39] G. Chatzikonstantinidis,[46] M. Chefdeville,[4] S. Chen,[55] S.-F. Cheung,[56] V. Chobanova,[38] M. Chrzaszcz,[41,27] X. Cid Vidal,[38] G. Ciezarek,[42] P. E. L. Clarke,[51] M. Clemencic,[39] H. V. Cliff,[48] J. Closier,[39] V. Coco,[58] J. Cogan,[6] E. Cogneras,[5] V. Cogoni,[16,j] L. Cojocariu,[30] G. Collazuol,[23,k] P. Collins,[39] A. Comerma-Montells,[12] A. Contu,[39] A. Cook,[47] S. Coquereau,[8] G. Corti,[39] M. Corvo,[17,a] C. M. Costa Sobral,[49] B. Couturier,[39] G. A. Cowan,[51] D. C. Craik,[51] A. Crocombe,[49] M. Cruz Torres,[61] S. Cunliffe,[54] R. Currie,[54] C. D'Ambrosio,[39] E. Dall'Occo,[42] J. Dalseno,[47] P. N. Y. David,[42] A. Davis,[58] O. De Aguiar Francisco,[2] K. De Bruyn,[6] S. De Capua,[55] M. De Cian,[12] J. M. De Miranda,[1] L. De Paula,[2] P. De Simone,[19] C.-T. Dean,[52] D. Decamp,[4] M. Deckenhoff,[10] L. Del Buono,[8] M. Demmer,[10] D. Derkach,[67] O. Deschamps,[5] F. Dettori,[39] B. Dey,[22] A. Di Canto,[39] H. Dijkstra,[39] F. Dordei,[39] M. Dorigo,[40] A. Dosil Suárez,[38] A. Dovbnya,[44] K. Dreimanis,[53] L. Dufour,[42] G. Dujany,[55] K. Dungs,[39] P. Durante,[39] R. Dzhelyadin,[36] A. Dziurda,[39] A. Dzyuba,[31] N. Déléage,[4] S. Easo,[50] U. Egede,[54] V. Egorychev,[32] S. Eidelman,[35] S. Eisenhardt,[51] U. Eitschberger,[10] R. Ekelhof,[10] L. Eklund,[52] Ch. Elsasser,[41] S. Ely,[60] S. Esen,[12] H. M. Evans,[48] T. Evans,[56] A. Falabella,[15] N. Farley,[46] S. Farry,[53] R. Fay,[53] D. Ferguson,[51] V. Fernandez Albor,[38] F. Ferrari,[15,39] F. Ferreira Rodrigues,[1] M. Ferro-Luzzi,[39] S. Filippov,[34] M. Fiore,[17,a] M. Fiorini,[17,a] M. Firlej,[28] C. Fitzpatrick,[40] T. Fiutowski,[28] F. Fleuret,[7,l] K. Fohl,[39] M. Fontana,[16] F. Fontanelli,[20,h] D. C. Forshaw,[60] R. Forty,[39] M. Frank,[39] C. Frei,[39] M. Frosini,[18] J. Fu,[22,m] E. Furfaro,[25,g] C. Färber,[39] A. Gallas Torreira,[38] D. Galli,[15,f] S. Gallorini,[23] S. Gambetta,[51] M. Gandelman,[2] P. Gandini,[56] Y. Gao,[3] J. García Pardiñas,[38] J. Garra Tico,[48] L. Garrido,[37] P. J. Garsed,[48] D. Gascon,[37] C. Gaspar,[39] L. Gavardi,[10] G. Gazzoni,[5] D. Gerick,[12] E. Gersabeck,[12] M. Gersabeck,[55] T. Gershon,[49] Ph. Ghez,[4] S. Gianì,[40] V. Gibson,[48] O. G. Girard,[40] L. Giubega,[30] K. Gizdov,[51] V. V. Gligorov,[8] D. Golubkov,[32] A. Golutvin,[54,39] A. Gomes,[1,n] I. V. Gorelov,[33] C. Gotti,[21,c] M. Grabalosa Gándara,[5] R. Graciani Diaz,[37] L. A. Granado Cardoso,[39] E. Graugés,[37] E. Graverini,[41] G. Graziani,[18] A. Grecu,[30] P. Griffith,[46] L. Grillo,[12] B. R. Gruberg Cazon,[56] O. Grünberg,[65] E. Gushchin,[34] Yu. Guz,[36] T. Gys,[39] C. Göbel,[61] T. Hadavizadeh,[56] C. Hadjivasiliou,[60] G. Haefeli,[40] C. Haen,[39] S. C. Haines,[48] S. Hall,[54] B. Hamilton,[59] X. Han,[12] S. Hansmann-Menzemer,[12] N. Harnew,[56] S. T. Harnew,[47] J. Harrison,[55] J. He,[62] T. Head,[40] A. Heister,[9] K. Hennessy,[53] P. Henrard,[5] L. Henry,[8] J. A. Hernando Morata,[38] E. van Herwijnen,[39] M. Heß,[65] A. Hicheur,[2] D. Hill,[56] C. Hombach,[55] W. Hulsbergen,[42] T. Humair,[54] M. Hushchyn,[67] N. Hussain,[56] D. Hutchcroft,[53] M. Idzik,[28] P. Ilten,[57] R. Jacobsson,[39] A. Jaeger,[12] J. Jalocha,[56] E. Jans,[42] A. Jawahery,[59] M. John,[56] D. Johnson,[39] C. R. Jones,[48] C. Joram,[39] B. Jost,[39] N. Jurik,[60] S. Kandybei,[44] W. Kanso,[6] M. Karacson,[39] J. M. Kariuki,[47] S. Karodia,[52] M. Kecke,[12] M. Kelsey,[60] I. R. Kenyon,[46] M. Kenzie,[39] T. Ketel,[43] E. Khairullin,[67] B. Khanji,[21,39,c] C. Khurewathanakul,[40] T. Kirn,[9] S. Klaver,[55] K. Klimaszewski,[29] S. Koliiev,[45] M. Kolpin,[12] I. Komarov,[40] R. F. Koopman,[43] P. Koppenburg,[42] A. Kozachuk,[33] M. Kozeiha,[5] L. Kravchuk,[34] K. Kreplin,[12] M. Kreps,[49]

P. Krokovny,[35] F. Kruse,[10] W. Krzemien,[29] W. Kucewicz,[27,o] M. Kucharczyk,[27] V. Kudryavtsev,[35] A. K. Kuonen,[40] K. Kurek,[29] T. Kvaratskheliya,[32,39] D. Lacarrere,[39] G. Lafferty,[55,39] A. Lai,[16] D. Lambert,[51] G. Lanfranchi,[19] C. Langenbruch,[49] B. Langhans,[39] T. Latham,[49] C. Lazzeroni,[46] R. Le Gac,[6] J. van Leerdam,[42] J.-P. Lees,[4] A. Leflat,[33,39] J. Lefrançois,[7] R. Lefèvre,[5] F. Lemaitre,[39] E. Lemos Cid,[38] O. Leroy,[6] T. Lesiak,[27] B. Leverington,[12] Y. Li,[7] T. Likhomanenko,[67,66] R. Lindner,[39] C. Linn,[39] F. Lionetto,[41] B. Liu,[16] X. Liu,[3] D. Loh,[49] I. Longstaff,[52] J. H. Lopes,[2] D. Lucchesi,[23,k] M. Lucio Martinez,[38] H. Luo,[51] A. Lupato,[23] E. Luppi,[17,a] O. Lupton,[56] A. Lusiani,[24] X. Lyu,[62] F. Machefert,[7] F. Maciuc,[30] O. Maev,[31] K. Maguire,[55] S. Malde,[56] A. Malinin,[66] T. Maltsev,[35] G. Manca,[7] G. Mancinelli,[6] P. Manning,[60] J. Maratas,[5] J. F. Marchand,[4] U. Marconi,[15] C. Marin Benito,[37] P. Marino,[24,i] J. Marks,[12] G. Martellotti,[26] M. Martin,[6] M. Martinelli,[40] D. Martinez Santos,[38] F. Martinez Vidal,[68] D. Martins Tostes,[2] L. M. Massacrier,[7] A. Massafferri,[1] R. Matev,[39] A. Mathad,[49] Z. Mathe,[39] C. Matteuzzi,[21] A. Mauri,[41] B. Maurin,[40] A. Mazurov,[46] M. McCann,[54] J. McCarthy,[46] A. McNab,[55] R. McNulty,[13] B. Meadows,[58] F. Meier,[10] M. Meissner,[12] D. Melnychuk,[29] M. Merk,[42] E Michielin,[23] D. A. Milanes,[64] M.-N. Minard,[4] D. S. Mitzel,[12] J. Molina Rodriguez,[61] I. A. Monroy,[64] S. Monteil,[5] M. Morandin,[23] P. Morawski,[28] A. Mordà,[6] M. J. Morello,[24,i] J. Moron,[28] A. B. Morris,[51] R. Mountain,[60] F. Muheim,[51] M. Mulder,[42] M. Mussini,[15] D. Müller,[55] J. Müller,[10] K. Müller,[41] V. Müller,[10] P. Naik,[47] T. Nakada,[40] R. Nandakumar,[50] A. Nandi,[56] I. Nasteva,[2] M. Needham,[51] N. Neri,[22] S. Neubert,[12] N. Neufeld,[39] M. Neuner,[12] A. D. Nguyen,[40] C. Nguyen-Mau,[40,p] V. Niess,[5] S. Nieswand,[9] R. Niet,[10] N. Nikitin,[33] T. Nikodem,[12] A. Novoselov,[36] D. P. O'Hanlon,[49] A. Oblakowska-Mucha,[28] V. Obraztsov,[36] S. Ogilvy,[19] R. Oldeman,[48] C. J. G. Onderwater,[69] J. M. Otalora Goicochea,[2] A. Otto,[39] P. Owen,[41] A. Oyanguren,[68] A. Palano,[14,q] F. Palombo,[22,m] M. Palutan,[19] J. Panman,[39] A. Papanestis,[50] M. Pappagallo,[52] L. L. Pappalardo,[17,a] C. Pappenheimer,[58] W. Parker,[59] C. Parkes,[55] G. Passaleva,[18] G. D. Patel,[53] M. Patel,[54] C. Patrignani,[15,f] A. Pearce,[55,50] A. Pellegrino,[42] G. Penso,[26,r] M. Pepe Altarelli,[39] S. Perazzini,[39] P. Perret,[5] L. Pescatore,[46] K. Petridis,[47] A. Petrolini,[20,h] A. Petrov,[66] M. Petruzzo,[22,m] E. Picatoste Olloqui,[37] B. Pietrzyk,[4] M. Pikies,[27] D. Pinci,[26] A. Pistone,[20] A. Piucci,[12] S. Playfer,[51] M. Plo Casasus,[38] T. Poikela,[39] F. Polci,[8] A. Poluektov,[49,35] I. Polyakov,[32] E. Polycarpo,[2] G. J. Pomery,[47] A. Popov,[36] D. Popov,[11,39] B. Popovici,[30] C. Potterat,[2] E. Price,[47] J. D. Price,[53] J. Prisciandaro,[38] A. Pritchard,[53] C. Prouve,[47] V. Pugatch,[45] A. Puig Navarro,[40] G. Punzi,[24,s] W. Qian,[56] R. Quagliani,[7,47] B. Rachwal,[27] J. H. Rademacker,[47] M. Rama,[24] M. Ramos Pernas,[38] M. S. Rangel,[2] I. Raniuk,[44] G. Raven,[43] F. Redi,[54] S. Reichert,[10] A. C. dos Reis,[1] C. Remon Alepuz,[68] V. Renaudin,[7] S. Ricciardi,[50] S. Richards,[47] M. Rihl,[39] K. Rinnert,[53,39] V. Rives Molina,[37] P. Robbe,[7,39] A. B. Rodrigues,[1] E. Rodrigues,[58] J. A. Rodriguez Lopez,[64] P. Rodriguez Perez,[55] A. Rogozhnikov,[67] S. Roiser,[39] V. Romanovskiy,[36] A. Romero Vidal,[38] J. W. Ronayne,[13] M. Rotondo,[23] T. Ruf,[39] P. Ruiz Valls,[68] J. J. Saborido Silva,[38] N. Sagidova,[31] B. Saitta,[16,j] V. Salustino Guimaraes,[2] C. Sanchez Mayordomo,[68] B. Sanmartin Sedes,[38] R. Santacesaria,[26] C. Santamarina Rios,[38] M. Santimaria,[19] E. Santovetti,[25,g] A. Sarti,[19,r] C. Satriano,[26,b] A. Satta,[25] D. M. Saunders,[47] D. Savrina,[32,33] S. Schael,[9] M. Schiller,[39] H. Schindler,[39] M. Schlupp,[10] M. Schmelling,[11] T. Schmelzer,[10] B. Schmidt,[39] O. Schneider,[40] A. Schopper,[39] M. Schubiger,[40] M.-H. Schune,[7] R. Schwemmer,[39] B. Sciascia,[19] A. Sciubba,[26,r] A. Semennikov,[32] A. Sergi,[46] N. Serra,[41] J. Serrano,[6] L. Sestini,[23] P. Seyfert,[21] M. Shapkin,[36] I. Shapoval,[17,44,a] Y. Shcheglov,[31] T. Shears,[53] L. Shekhtman,[35] V. Shevchenko,[66] A. Shires,[10] B. G. Siddi,[17] R. Silva Coutinho,[41] L. Silva de Oliveira,[2] G. Simi,[23,k] M. Sirendi,[48] N. Skidmore,[47] T. Skwarnicki,[60] E. Smith,[54] I. T. Smith,[51] J. Smith,[48] M. Smith,[55] H. Snoek,[42] M. D. Sokoloff,[58] F. J. P. Soler,[52] D. Souza,[47] B. Souza De Paula,[2] B. Spaan,[10] P. Spradlin,[52] S. Sridharan,[39] F. Stagni,[39] M. Stahl,[12] S. Stahl,[39] P. Stefko,[40] S. Stefkova,[54] O. Steinkamp,[41] O. Stenyakin,[36] S. Stevenson,[56] S. Stoica,[30] S. Stone,[60] B. Storaci,[41] S. Stracka,[24,i] M. Straticiu,[30] U. Straumann,[41] L. Sun,[58] W. Sutcliffe,[54] K. Swientek,[28] V. Syropoulos,[43] M. Szczekowski,[29] T. Szumlak,[28] S. T'Jampens,[4] A. Tayduganov,[6] T. Tekampe,[10] G. Tellarini,[17,a] F. Teubert,[39] C. Thomas,[56] E. Thomas,[39] J. van Tilburg,[42] V. Tisserand,[4] M. Tobin,[40] S. Tolk,[48] L. Tomassetti,[17,a] D. Tonelli,[39] S. Topp-Joergensen,[56] E. Tournefier,[4] S. Tourneur,[40] K. Trabelsi,[40] M. Traill,[52] M. T. Tran,[40] M. Tresch,[41] A. Trisovic,[39] A. Tsaregorodtsev,[6] P. Tsopelas,[42] A. Tully,[48] N. Tuning,[42] A. Ukleja,[29] A. Ustyuzhanin,[67,66] U. Uwer,[12] C. Vacca,[16,39,j] V. Vagnoni,[15,39] S. Valat,[39] G. Valenti,[15] A. Vallier,[7] R. Vazquez Gomez,[19] P. Vazquez Regueiro,[38] S. Vecchi,[17] M. van Veghel,[42] J. J. Velthuis,[47] M. Veltri,[18,t] G. Veneziano,[40] A. Venkateswaran,[60] M. Vesterinen,[12] B. Viaud,[7] D. Vieira,[1] M. Vieites Diaz,[38] X. Vilasis-Cardona,[37,e] V. Volkov,[33] A. Vollhardt,[41] B Voneki,[39] D. Voong,[47] A. Vorobyev,[31] V. Vorobyev,[35] C. Voß,[65] J. A. de Vries,[42] C. Vázquez Sierra,[38] R. Waldi,[65] C. Wallace,[49] R. Wallace,[13] J. Walsh,[24] J. Wang,[60] D. R. Ward,[48] H. M. Wark,[53] N. K. Watson,[46] D. Websdale,[54] A. Weiden,[41] M. Whitehead,[39] J. Wicht,[49] G. Wilkinson,[56,39] M. Wilkinson,[60] M. Williams,[39] M. P. Williams,[46] M. Williams,[57] T. Williams,[46] F. F. Wilson,[50] J. Wimberley,[59] J. Wishahi,[10] W. Wislicki,[29] M. Witek,[27] G. Wormser,[7] S. A. Wotton,[48]

K. Wraight,[52] S. Wright,[48] K. Wyllie,[39] Y. Xie,[63] Z. Xing,[60] Z. Xu,[40] Z. Yang,[3] H. Yin,[63] J. Yu,[63] X. Yuan,[35] O. Yushchenko,[36] M. Zangoli,[15] K. A. Zarebski,[46] M. Zavertyaev,[11,u] L. Zhang,[3] Y. Zhang,[7] Y. Zhang,[62] A. Zhelezov,[12] Y. Zheng,[62] A. Zhokhov,[32] V. Zhukov,[9] and S. Zucchelli[15]

(LHCb Collaboration)

[1]*Centro Brasileiro de Pesquisas Físicas (CBPF), Rio de Janeiro, Brazil*
[2]*Universidade Federal do Rio de Janeiro (UFRJ), Rio de Janeiro, Brazil*
[3]*Center for High Energy Physics, Tsinghua University, Beijing, China*
[4]*LAPP, Université Savoie Mont-Blanc, CNRS/IN2P3, Annecy-Le-Vieux, France*
[5]*Clermont Université, Université Blaise Pascal, CNRS/IN2P3, LPC, Clermont-Ferrand, France*
[6]*CPPM, Aix-Marseille Université, CNRS/IN2P3, Marseille, France*
[7]*LAL, Université Paris-Sud, CNRS/IN2P3, Orsay, France*
[8]*LPNHE, Université Pierre et Marie Curie, Université Paris Diderot, CNRS/IN2P3, Paris, France*
[9]*I. Physikalisches Institut, RWTH Aachen University, Aachen, Germany*
[10]*Fakultät Physik, Technische Universität Dortmund, Dortmund, Germany*
[11]*Max-Planck-Institut für Kernphysik (MPIK), Heidelberg, Germany*
[12]*Physikalisches Institut, Ruprecht-Karls-Universität Heidelberg, Heidelberg, Germany*
[13]*School of Physics, University College Dublin, Dublin, Ireland*
[14]*Sezione INFN di Bari, Bari, Italy*
[15]*Sezione INFN di Bologna, Bologna, Italy*
[16]*Sezione INFN di Cagliari, Cagliari, Italy*
[17]*Sezione INFN di Ferrara, Ferrara, Italy*
[18]*Sezione INFN di Firenze, Firenze, Italy*
[19]*Laboratori Nazionali dell'INFN di Frascati, Frascati, Italy*
[20]*Sezione INFN di Genova, Genova, Italy*
[21]*Sezione INFN di Milano Bicocca, Milano, Italy*
[22]*Sezione INFN di Milano, Milano, Italy*
[23]*Sezione INFN di Padova, Padova, Italy*
[24]*Sezione INFN di Pisa, Pisa, Italy*
[25]*Sezione INFN di Roma Tor Vergata, Roma, Italy*
[26]*Sezione INFN di Roma La Sapienza, Roma, Italy*
[27]*Henryk Niewodniczanski Institute of Nuclear Physics Polish Academy of Sciences, Kraków, Poland*
[28]*AGH—University of Science and Technology, Faculty of Physics and Applied Computer Science, Kraków, Poland*
[29]*National Center for Nuclear Research (NCBJ), Warsaw, Poland*
[30]*Horia Hulubei National Institute of Physics and Nuclear Engineering, Bucharest-Magurele, Romania*
[31]*Petersburg Nuclear Physics Institute (PNPI), Gatchina, Russia*
[32]*Institute of Theoretical and Experimental Physics (ITEP), Moscow, Russia*
[33]*Institute of Nuclear Physics, Moscow State University (SINP MSU), Moscow, Russia*
[34]*Institute for Nuclear Research of the Russian Academy of Sciences (INR RAN), Moscow, Russia*
[35]*Budker Institute of Nuclear Physics (SB RAS) and Novosibirsk State University, Novosibirsk, Russia*
[36]*Institute for High Energy Physics (IHEP), Protvino, Russia*
[37]*Universitat de Barcelona, Barcelona, Spain*
[38]*Universidad de Santiago de Compostela, Santiago de Compostela, Spain*
[39]*European Organization for Nuclear Research (CERN), Geneva, Switzerland*
[40]*Ecole Polytechnique Fédérale de Lausanne (EPFL), Lausanne, Switzerland*
[41]*Physik-Institut, Universität Zürich, Zürich, Switzerland*
[42]*Nikhef National Institute for Subatomic Physics, Amsterdam, The Netherlands*
[43]*Nikhef National Institute for Subatomic Physics and VU University Amsterdam, Amsterdam, The Netherlands*
[44]*NSC Kharkiv Institute of Physics and Technology (NSC KIPT), Kharkiv, Ukraine*
[45]*Institute for Nuclear Research of the National Academy of Sciences (KINR), Kyiv, Ukraine*
[46]*University of Birmingham, Birmingham, United Kingdom*
[47]*H.H. Wills Physics Laboratory, University of Bristol, Bristol, United Kingdom*
[48]*Cavendish Laboratory, University of Cambridge, Cambridge, United Kingdom*
[49]*Department of Physics, University of Warwick, Coventry, United Kingdom*
[50]*STFC Rutherford Appleton Laboratory, Didcot, United Kingdom*
[51]*School of Physics and Astronomy, University of Edinburgh, Edinburgh, United Kingdom*
[52]*School of Physics and Astronomy, University of Glasgow, Glasgow, United Kingdom*
[53]*Oliver Lodge Laboratory, University of Liverpool, Liverpool, United Kingdom*

[54]Imperial College London, London, United Kingdom
[55]School of Physics and Astronomy, University of Manchester, Manchester, United Kingdom
[56]Department of Physics, University of Oxford, Oxford, United Kingdom
[57]Massachusetts Institute of Technology, Cambridge, Massachusetts, United States
[58]University of Cincinnati, Cincinnati, Ohio, United States
[59]University of Maryland, College Park, Maryland, United States
[60]Syracuse University, Syracuse, New York, United States
[61]Pontifícia Universidade Católica do Rio de Janeiro (PUC-Rio), Rio de Janeiro, Brazil associated with Universidade Federal do Rio de Janeiro (UFRJ), Rio de Janeiro, Brazil
[62]University of Chinese Academy of Sciences, Beijing, China associated with Center for High Energy Physics, Tsinghua University, Beijing, China
[63]Institute of Particle Physics, Central China Normal University, Wuhan, Hubei, China associated with Center for High Energy Physics, Tsinghua University, Beijing, China
[64]Departamento de Fisica, Universidad Nacional de Colombia, Bogota, Colombia associated with LPNHE, Universite Pierre et Marie Curie, Universite Paris Diderot, CNRS/IN2P3, Paris, France
[65]Institut für Physik, Universität Rostock, Rostock, Germany associated with Physikalisches Institut, Ruprecht-Karls-Universitat Heidelberg, Heidelberg, Germany
[66]National Research Centre Kurchatov Institute, Moscow, Russia associated with Institute of Theoretical and Experimental Physics 15 (ITEP), Moscow, Russia
[67]Yandex School of Data Analysis, Moscow, Russia associated with Institute of Theoretical and Experimental Physics (ITEP), Moscow, Russia
[68]Instituto de Fisica Corpuscular (IFIC), Universitat de Valencia-CSIC, Valencia, Spain associated with Universitat de Barcelona, Barcelona, Spain
[69]Van Swinderen Institute, University of Groningen, Groningen, The Netherlands associated with Nikhef National Institute for Subatomic Q7 Physics, Amsterdam, The Netherlands

[a]Also at Universidade Federal do Triângulo Mineiro (UFTM), Uberaba-MG, Brazil.
[b]Also at Università di Roma La Sapienza, Roma, Italy.
[c]Also at Università della Basilicata, Potenza, Italy.
[d]Also at Università di Urbino, Urbino, Italy.
[e]Also at Università di Ferrara, Ferrara, Italy.
[f]Also at P.N. Lebedev Physical Institute, Russian Academy of Science (LPI RAS), Moscow, Russia.
[g]Also at Università di Bari, Bari, Italy.
[h]Also at Università degli Studi di Milano, Milano, Italy.
[i]Also at Università di Roma Tor Vergata, Roma, Italy.
[j]Also at Scuola Normale Superiore, Pisa, Italy.
[k]Also at Università di Milano Bicocca, Milano, Italy.
[l]Also at Hanoi University of Science, Hanoi, Viet Nam.
[m]Also at Università di Padova, Padova, Italy.
[n]Also at AGH—University of Science and Technology, Faculty of Computer Science, Electronics and Telecommunications, Kraków, Poland.
[o]Also at Università di Cagliari, Cagliari, Italy.
[p]Also at Università di Genova, Genova, Italy.
[q]Also at Laboratoire Leprince-Ringuet, Palaiseau, France.
[r]Also at Università di Bologna, Bologna, Italy.
[s]Also at Università di Modena e Reggio Emilia, Modena, Italy.
[t]Also at Università di Pisa, Pisa, Italy.
[u]Also at LIFAELS, La Salle, Universitat Ramon Llull, Barcelona, Spain.